Fast Ion power loads on ITER First Wall Structures in the Presence of NTMs and microturbulence

T. Kurki-Suonio[1], O. Asunta[1], T. Koskela[1], A. Snicker[1], T. Hauff[2], F. Jenko[2], E. Poli[2], and S. Sipilä[1]

[1]*Aalto University, Assn Euratom-Tekes, P.O. Box 14100, FI-00076 AALTO, Finland*
[2]*Max-Planck-Institut für Plasmaphysik, EURATOM Association Boltzmannstrasse 2, D-85748 Garching, Germany*

1 Introduction

The new physics introduced by ITER operation is related to the very energetic (3.5 MeV) alpha particles produced in large quantities in fusion reactions. These particles not only constitute a massive energy source inside the plasma, but they also present a potential hazard to the material structures that provide the containment of the burning plasma. In addition, the negative neutral beam injection produces 1 MeV deuterons and application of ICRH minority ions in multi-MeV range.

The finite number (18 in ITER) and limited toroidal extent of the Toroidal Field (TF) coils cause a periodic variation of the toroidal field called the magnetic ripple. This ripple can provide a significant channel for fast particle leakage, leading to very localized fast particle loads on the walls. Because the ripple could cause significant additional ion transport, ferromagnetic inserts (FIs), will be embedded in the double wall structure of the ITER vacuum vessel in order to reduce the ripple. In ITER the toroidal field deviations are locally further enhanced by the presence of discrete ferromagnetic structures, e.g. the test blanket modules (TBMs), that cause poloidally and toroidally localized perturbations to the magnetic field.

We have already carried out a preliminary study of the wall loads caused by three types of fast particles; fusion-born alpha particles, deuterons from neutral beam injection (NBI), and ICRH-heated minority ions, in a variety of ITER plasmas using the 5D Monte Carlo guiding-center code ASCOT [1]. The simulations were performed for different magnetic field configurations including FIs and none or more TBMs. The simulations were carried out using input data that has later been either changed (the wall structure and geometry of FIs) or found deficient (the 3D magnetic background corresponding to the situation with TBMs).

All the simulations thus far have been based on the assumption that the fast ion transport is dominated by neoclassical effects. In MHD quiescent plasmas this was believed to be true until the first NBI current drive experiments with the ASDEX Upgrade tangential beams failed to demonstrate the predicted levels of off-axis current [2]. Subsequent theoretical work has revealed that, unlike previously believed, microturbulence can induce additional transport of not just the bulk plasma but also the fast ions [3]. Furthermore, it is highly unlikely that the ITER plasmas will be MHD quiescent: the massive fast ion population consisting of the fusion alphas with energies up to 3.5 MeV drive a multitude of Alfvénic modes and other energetic particle modes which, in turn, act back to the fast ion population. Furthermore, ITER is prone to Neoclassical Tearing Modes (NTMs)

with substantial island structures. All these MHD phenomena can contribute to increased transport of fast ions in the core plasma. This in turn increases the fast ion population at the edge where the transport due to the field aberrations caused by toroidal field coils and TBMs can lead to unacceptably high peak power loads on some first wall components. None of the guiding-center codes presently in use worldwide can account for all these effects.

We have started incorporating effects of plasma instabilities on transport into ASCOT. It now has a theory-based model for anomalous diffusion due to microturbulence [3] and a model of magnetic islands due to NTMs [4, 5]. In this paper we present the first simulation results of fast ion power loads to ITER plasma-facing components with a realistic 3D magnetic field, the most recent 3D wall structure, and taking into account the fast ion redistribution due to microturbulence and NTMs. Unfortunately, as yet we cannot report on the combined effect of NTMs and TBMs.

2 Numerical model for islands in ASCOT

Instead of trying to incorporate island structures in the components of the magnetic background field, we have adopted another approach [4]. We use relativistic Hamiltonian formalism in deriving the equation of motion in magnetic coordinates and add the effect of magnetic islands as a perturbation in the magnetic vector potential as in [4]. The perturbation describing NTMs is given by [6]:

$$\alpha(\chi, \theta, \zeta, t) = \sum_{n,m} A_{m,n}(\chi) \cos(m\theta - n\zeta),\qquad(1)$$

where the amplitudes $A_{m,n}$ for different perturbations can be functions of the radial coordinate χ, m is the poloidal mode number and n is the toroidal mode number. In ASCOT, we use the normalized poloidal flux ψ_n as a radial coordinate. For the radial profile $A_{m,n}$ we use a theory-based parametrization [7] describing resistive modes

$$A_{m,n}(\chi) = \rho_{m,n}\alpha \left(\frac{\chi}{\chi_{m,n}}\right)^{m/2} \left(1 - \beta\left(\frac{\chi}{\chi_{m,n}}\right)^{1/2}\right) \text{ ,for } \chi \leq \chi_{m,n}$$

$$A_{m,n}(\chi) = \rho_{m,n}\frac{\alpha(1-\beta) - \gamma + \gamma\left(\frac{\chi}{\chi_{m,n}}\right)^{1/2}}{(\chi/\chi_{m,n})^{(m+1)/2}} \text{ ,for } \chi > \chi_{m,n}.\qquad(2)$$

The parameters $\rho_{m,n}$, α, β and γ are fixed so that the island width, measured by electron cyclotron emission (ECE), the island position (ECE or soft X-ray SXR) and the radial perturbation field strength (Mirnov coils), correspond to the ones obtained from experimental data.

The model has been tested and found to give physically reasonable island structures that are observable in particle orbits. Preliminary ASCOT results on fast ion confinement using this model were reported in EPS 2010 [8]. Figure 1 shows the island structures used in this work.
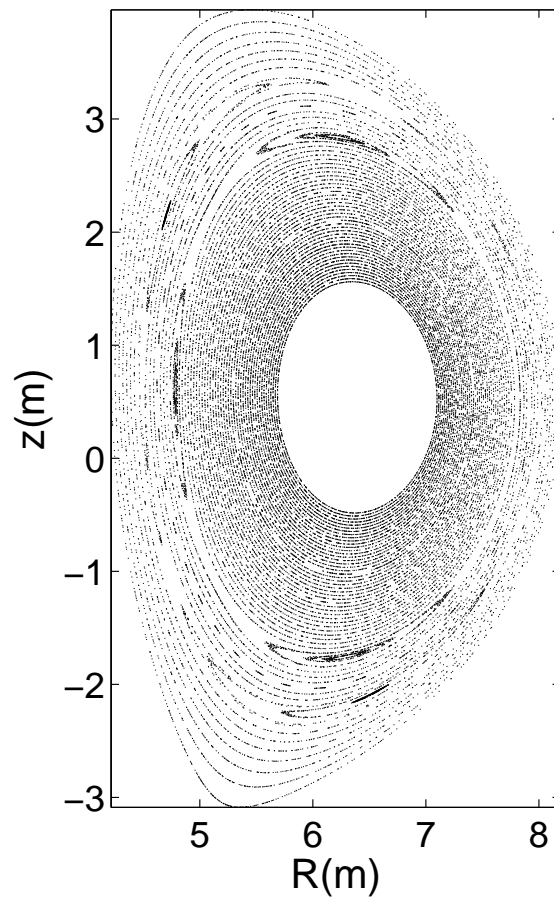
Figure 1: A Poincaré plot of (3,2) and (2,1) perturbations at $\phi = 0$ in ITER.

3 Numerical model for turbulent diffusion of fast ions in ASCOT

Until now ASCOT, like most other guiding centre codes attempting to include anomalous effects, have used diffusion coefficients D that are either constants or exhibit some radial and/or energy dependence that is included on ad hoc basis. Recently a more theory-based model for the diffusion coefficient has been published [3], where the value of the diffusion coefficient derives from the properties of the plasma background and the resulting micro-turbulence. Both electrostatic and electromagnetic turbulence were addressed, and the corresponding diffusion coefficients, D_E and D_B, were calculated separately for strongly trapped and strongly passing orbits. According to the model, the effect of turbulence does not fall off as rapidly with energy as previously thought. Rather, in the case of electrostatic turbulence the anomalous diffusion falls off only as $E^{-0.5\cdots-1.0}$ ($E^{-0.5}$ for small and $E^{-1.0}$ for large pitch angles), and in the case of magnetic turbulence as $E^{-0.5...0.0}$. We have now implemented this numerical diffusion model into ASCOT in order to get more realistic values for not only the peak power loads on ITER walls but for the neutral beam driven current as well.

The traditional way of incorporating non-neoclassical transport effects into guiding centre simulations is based on the work by Boozer and Kuo-Petravic [9]. They used a diffusion equation,

$$\frac{\partial f}{\partial t} = \frac{1}{s(\psi)} \frac{\partial}{\partial \psi} \left[sD \frac{\partial f}{\partial \psi} \right], \tag{3}$$

derived from the 3-dimensional Fick's law. Here ψ is a radial coordinate and $s(\psi)$ is defined so that the volume element of physical space is $d^3x = s(\psi)\, d\psi$. In this manner the diffusion coefficient D is given in its natural units $[D] = \mathrm{m}^2/\mathrm{s}$.

In ASCOT, diffusion is modelled with a Monte Carlo operator for the radial displacement $\Delta\rho$ in time step Δt:

$$\Delta\rho = \frac{\mathrm{d}}{\mathrm{dt}} \langle \psi \rangle \Delta t + \delta \sqrt{\frac{\mathrm{d}}{\mathrm{dt}} \left(\langle \psi^2 \rangle - \langle \psi \rangle^2 \right) \Delta t} \tag{4}$$

$$= \left\langle \frac{1}{s} \frac{\partial}{\partial \psi} (sD) \right\rangle \Delta t + \delta \sqrt{2 \langle D \rangle \Delta t}. \tag{5}$$

The first, deterministic term gives the mean drift velocity. The second, stochastic term, where $\delta = \pm 1$ is a random sign, generates the desired standard deviation to the distribution. The deterministic term seems to be typically at least an order of magnitude smaller than the stochastic term but, due to its cumulative nature, it can still play an important role in longer simulations.

Initially, Hauff et al. derived the model only for strongly passing and strongly trapped particles [3]. For ASCOT simulations, however, expressions for the diffusion coefficients that are valid for all orbit topologies are needed. The published diffusion coefficients have been extended to arbitrary values of the particle pitch $\xi \equiv v_\parallel/v$ and to both large and small gyro-radii in Ref. [10]. In addition to the pitch dependence, the diffusion coefficients explicitly depend on the particle energy. The microturbulence enters the diffusion coefficients in the form of correlation lengths and, in the case of electrostatic turbulence,
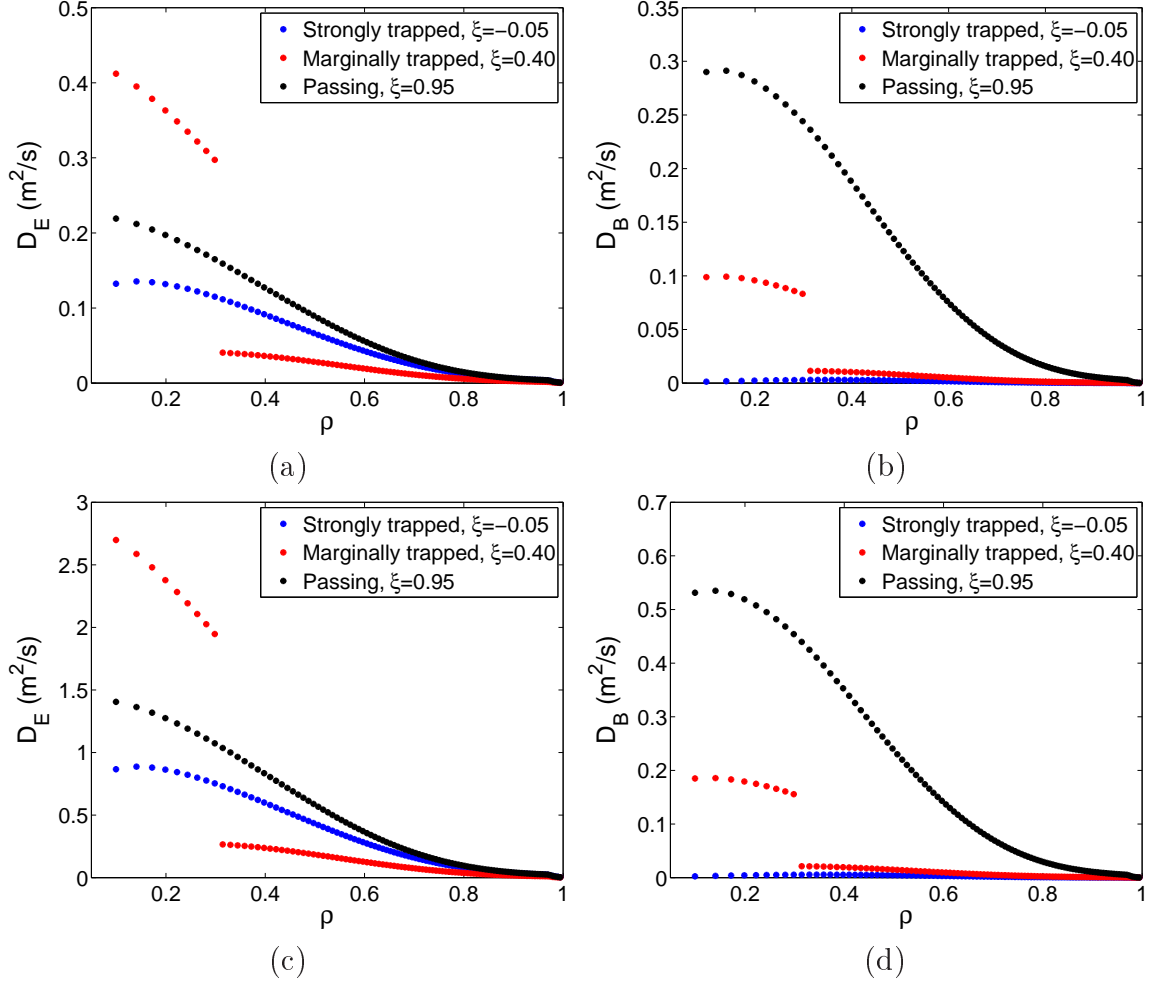
Figure 2: *Radial profiles of (a) D_E and (b) D_B for three extreme alpha particle orbits. Similar plots for a 1.0 MeV deuteron, (c) and (d), demonstrate the energy dependencies in anomalous transport due to electrostatic and magnetic turbulence. The discontinuity in the diffusion coefficient corresponding to the marginally trapped orbit is due to the change in orbit topology at that radius.*

the $\mathbf{E} \times \mathbf{B}$ velocity. Also the plasma background, in the form of local temperature values, enters the equations for the diffusion coefficients.

For example, the largest diffusion coefficient in the case of 3.5 MeV alphas (i.e. large Larmor radius) is due to electrostatic turbulence and it can be written as

$$D_{large\rho} \approx \frac{1.73 \hat{V}_E^2 \hat{\lambda}_c \hat{\lambda}_V}{12 \sqrt{\pi (1 - \xi^2)} \xi^2} \left(\frac{E}{T_e} \right)^{-3/2} \frac{\rho_i^2 c_i}{R_0} \tag{6}$$

for passing particles, and

$$D_{large\rho} \approx \frac{1.73 \hat{V}_E^2 \hat{\lambda}_c \hat{\lambda}_V \sqrt{\epsilon}}{12 \sqrt{\pi} \xi (1 - \xi^2)} \left(\frac{E}{T_e} \right)^{-3/2} \frac{\rho_i^2 c_i}{R_0} \tag{7}$$

for trapped particles. Here T_e stands for the local electron temperature, ρ_i and c_i are thermal ion Larmor radius and sound speed, respectively. The radial dependence is via these local parameters. The values for the turbulence quantities, the mean magnitude of

the radial component of the $\mathbf{E} \times \mathbf{B}$ drift and the normalized electrostatic potential and $\mathbf{E} \times \mathbf{B}$ correlation lengths, $\hat{\lambda}_c$ and $\hat{\lambda}_V$, respectively, should be determined from experiments or turbulence simulations.

Experimentally the radial correlation lengths have been measured to be in the range $5 \ldots 10 \ \rho_s$ [11], while simulations of ITG and TEM turbulence have yielded the value $\lambda_c \sim 6\rho_s$.

Since the fundamental mechanism by which the diffusion operates is $\mathbf{E} \times \mathbf{B}$ drift, energy should be (approximately) conserved leaving one degree of freedom in how it is distributed among $v_\parallel$ and $v_\perp$. Currently the operator keeps both of them constant.

Figure 2 displays the radial profiles of D_E and D_B both a 3.5 MeV alpha and a 1 MeV NBI deuteron. Since the diffusion coefficients are pitch dependent, the diffusion coefficients are calculated for three extreme orbit topologies: (i) strongly passing ($\xi = 0.95$, small Larmor radius), (ii) strongly trapped ($\xi = -0.05$, large Larmor radius), and (iii) 'marginally trapped' orbit ($\xi = 0.40$, large banana orbit width). The term 'marginally trapped' should be taken with a grain of salt because, for a given particle pitch, the orbit is marginally trapped only in some part of the plasma. The anomalous diffusion is clearly more significant for the NBI deuterons than for the fusion alphas. It is also obvious that while the energy scaling of the anomalous diffusion due to magnetic turbulence is more worrisome, its absolute values generally remain small compared to that due to electrostatic turbulence. Another interesting observation is that the anomalous diffusion is largest for passing orbits.

4   Simulation results

The simulations should be carried out for two different ITER plasmas: Scenario 2, which is a standard H-mode, and Scenario 4, which corresponds to steady-state operation. In the earlier, neoclassical study, the wall power loads were found insignificant in Scenario 4 and much larger but still easily tolerable even in Scenario 2. The difference arises from the different plasma profiles: in Scenario 4, temperature and density profiles are much steeper, which causes thermal fusions and ionization of NBI particles to occur only close to the plasma core. Therefore it is expected that the redistribution of fast ions due to non-neoclassical effects can be particularly treacherous in Scenario 4: drift islands and anomalous transport lead energetic ions to the edge where ripple induced transport processes rapidly take them to the first wall components. However, due to space limitations we shall here focus only on fusion alphas in Scenario-2 which, when including also thermal load on the wall, is likely to have higher total power fluxes to the PFCs.

As described in Sec. 2, at present the numerical model for magnetic islands in ASCOT operates in Boozer coordinates that can be applied only in axisymmetric situations. Therefore, in this contribution, we can only combine the island structures with anomalous transport. However, an alternative approach to magnetic islands, where the island structures are incorporated in the background field, is currently under work, and the total effect of islands, turbulent transport and 3D field aberrations will be reported in a more

(a)   (b)
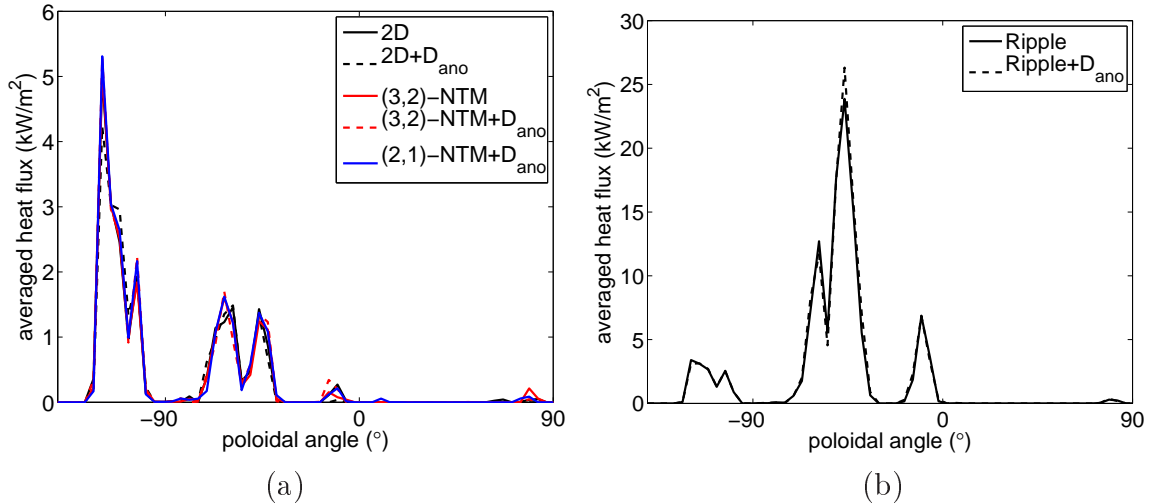
Figure 3: Toroidally averaged wall loads in (a) axisymmetric and (b) non-axisymmetric cases. The poloidal angle of 100 ∘ corresponds to the divertor. In axisymmetric case the peak power load is thus at the divertor, but including non-axisymmetry moves the peak to the poloidally extended limiters.

comprehensive publication to follow.

ITER wall design has undergone several revisions due to the strong geometrical constraints imposed on the location of the ferritic inserts as well as due to financial constraints. Our earlier studies reported on the power loads on a first wall with two limiters, but in this contribution we focus on a more recent design with a limiter-like structure in every coil period. The maximum ripple strength along the separatrix is 1.1%.

Figure 3(a) shows the toroidally averaged wall load due to fusion alphas in Scenario 2 for four different cases: pure neoclassical transport (black), add only turbulent diffusion (red), add only a (2,1) island (green), add only a (3,2) island (orange), and include both a (2,1) and a (3,2) island as well as turbulent diffusion. The island structures are illustrated in Fig. 1 and the turbulent diffusion coefficient in Fig. 2. The effect of ripple on fusion alphas in MHD-quiescent plasmas in the absence (green) and presence (red) of turbulent diffusion is shown in Fig. 3(b). These simulations were carried out using ITER wall design with 18 limiters so the toroidally averaged power load should give a good indication also of the peak power fluxes to the wall. However, if ITER adopts a smaller number of limiters, the situation is naturally quite different. This is illustrated in Fig. 4, where a 2-dimensional plot of the power flux to the wall is shown for the 18 limiters and for the earlier wall construction with only two limiters. Comments?

5   Conclusions

Preliminary results indicate that when ripple is not taken into account both the islands and anomalous diffusion have little effect on the wall loads. However, together with ripple, large islands increase the wall loads significantly. Luckily most of the load is still found on the limiters. The effect of anomalous diffusion on the wall loads is small compared to that of the islands.
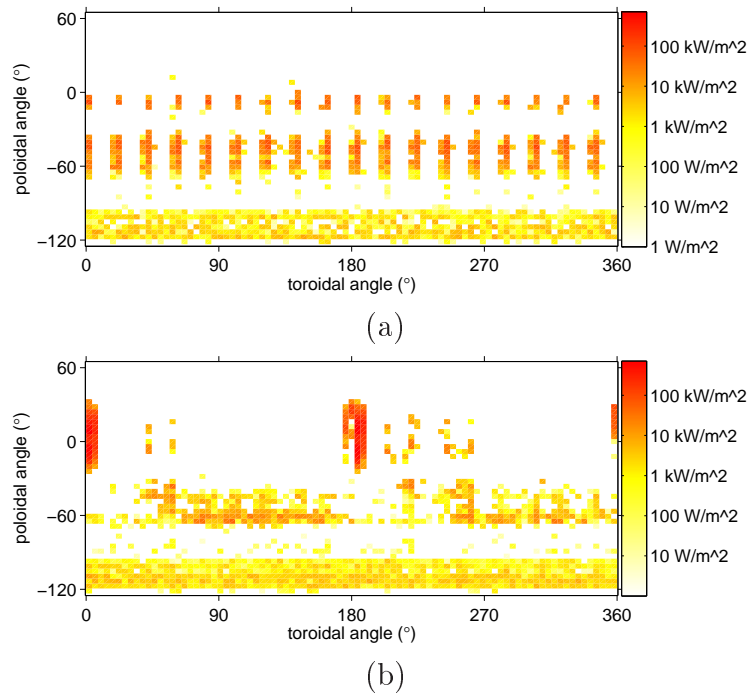
Figure 4: The power load density on the PFCs for two different wall designs: (a) wall with 18 poloidal limiters separated by 20° in toroidal angle and (b) wall with two port limiters located at toroidal angles 0° and 180°. Note the logarithmic color scale.

References

[1] T. Kurki-Suonio *et al.*, Nucl. Fusion **49** (2009) 095001

[2] S. Gunter *et al.*, Nucl. Fusion **47** (2007) 920

[3] T. Hauff, M. J. Pueschel, T. Dannert, and F. Jenko, Phys. Rev. Lett. **102** (2009) 075004

[4] S.D. Pinches *et al.*, Comp. Phys. Comm. **111** (1998) 133

[5] R.B. White and M.S. Chance, Phys. Fluids **27** (1984) 2455

[6] E. Strumberger *et al.*, New Journal of Physics **10** (2008) 023017

[7] V. Igochine *et al.*, Nucl. Fusion **46** (2006) 741

[8] A. Snicker *et al.*, P5.187, 37th EPS Conference on Plasma Physics, Dublin, Ireland, 21-25 June 2010

[9] A.H. Boozer and G. Kuo-Petravic, Phys. Fluids, **24** (1981) 851

[10] T. Hauff, Transport of Energetic Particles in Turbulent Plasmas, PhD. thesis, Universität Ulm, Ulm, Germany (2009)

[11] T.L. Rhodes, Phys. Plasmas **9** (2002) 2141